Journal of African Earth Sciences 124 (2016) 323–339

Contents lists available at ScienceDirect

Journal of African Earth Sciences

journal homepage: www.elsevier.com/locate/jafrearsci

Morphodynamic changes as an impact of human intervention at the Ras El-Bar-Damietta Harbor coast, NW Damietta Promontory, Nile Delta, Egypt

Hesham M. El-Asmar [a, b, *], Maysa M.N. Taha [c], Abdelbaset S. El-Sorogy [d, e]

[a] Academic and Education Affairs, King Saud University, Riyadh, 11451, Saudi Arabia
[b] Department of Geology, Faculty of Science, Damietta University, New Dameitta City, 34517, Egypt
[c] Geology Department, Faculty of Science, Helwan University, Egypt
[d] Department of Geology and Geophysics, College of Science, King Saud University, Saudi Arabia
[e] Geology Department, Faculty of Science, Zagazig University, Egypt

ARTICLE INFO

Article history:
Received 10 April 2016
Received in revised form
17 September 2016
Accepted 28 September 2016
Available online 28 September 2016

Keywords:
Beach
Geomorphology
Dynamic
Human impact
Ras El-Bar
Damietta Harbor
Nile Delta

ABSTRACT

Due to the absence of a national strategic plan for coastal management, the Nile Delta coast is no longer described as a fully dissipative, divergent, low-gradient beach face composed of fine to very fine sand. Instead, new patterns have emerged depending on rock type, geomorphology of the coast, direction of the shoreline in relation to waves and current, and the implemented defense measures. This study attempts to record the morphodynamic changes which occurred due to human intervention. Landsat satellite images acquired for the periods of time of 1973, 1984, 1989, 2003, and 2015 are used together with geomorphologic observations in order to monitor the changes along the coastal strip between Ras El-Bar and Damietta Harbor. This study reveals two beach segments; one of which lies to the east, it is protected with detached breakwater system, and shows average shoreline accretions of +4.73 myr^{-1}, +5.0 myr^{-1}, and +0.89myr^{-1} during the periods of 1984–1998, 1998–2003, and 2003–2015 respectively. This segment still has the geomorphologic imprints of the dissipative beach, wave divergence, low-gradient beach face, fine grained sand and spilling breakers. The second is to the west, between the detached breakwaters and the eastern jetty of the Damietta Harbor. It is an erosional segment with shoreline retreat of −7.43 myr^{-1}, −10.90 myr^{-1}, and −3.11myr^{-1} for the same periods. This segment shows intermediate "d" beach or intermediate-reflective, wave convergence, rip currents, with the characteristic steep sloped and cuspate beach face, cliffy, reworked sediments of coarse grained sands, mud clasts, discoidal gravels, shelly beach, and plunging breakings. The presence of convergent waves along this segment confirms the concept of an emergence of a new wave pattern of reversed eddy which enhances the steepness of the beach face, accelerates erosion, and increases the possibility of drowning of swimmers at Ras El-Bar resort. Under such circumstances the plunge step approaches the shore and its shell content forced by wave to accumulate forming the shelly beach. To secure the coastal strip against erosion and sea level changes the detached breakwaters should be extended to reach the eastern jetty of the Damietta Harbor. The protection of this segment is a matter of interest for investment projects related to industries and trading along the Damietta Harbor as well as the touristic investments at Ras El-Bar, as one of the important tourist destinations in Egypt. Millions of pounds spent by beach visitors and investment annually provide significant input to local and regional economy. Hazards associated with the morphodynamic effects on recreational beaches can influence the suitably of any given stretch of coast as a recreational resource, and thus impact tourist money spent in addition to the safety and well-being of beach visitors.

1. Introduction

The annual amount of sediment discharged by the Nile River at Aswan was calculated in the range of 160 × 10^{12} m^3 yr^{-1} (Sestini,

* Corresponding author. Academic and Education Affairs, King Saud University, Riyadh, 11451, Saudi Arabia.
E-mail address: hmelasmar@yahoo.com (H.M. El-Asmar).

http://dx.doi.org/10.1016/j.jafrearsci.2016.09.035
1464-343X/

1989). Aswan High Dam, completed in 1964, was built to control the flow of the Nile, to generate electricity and to provide water for irrigation. However, the dam has also impacted the sediment flux; amounts of sediment delivered at the river mouths of Rosetta and Damietta range between 100–115 $\times$ 10^6 m^3yr^{-1} (El-Dardir, 1994; Frihy and Lawrence, 2004) are no longer sufficient to nourish the Nile Delta coastline and prevent coastal erosion (Orlova and Zenkovich, 1974; Smith and Abdel Kader, 1988; Lotfy and Frihy, 1993; Stanley, 1996). As a result, a great deal of effort has been expended on construction of coastal defense structures to protect sections of the coast of particular socioeconomic importance, such as recreational beaches (El-Asmar, 2002), and new communities and harbors (White and El-Asmar, 1999; El-Asmar and White, 2002). Due in part to the absence of a unified strategy for protecting the whole Nile Delta coast, contemporary erosion of the coastline threatens to become a major environmental hazard (White and El-Asmar, 1999).

In Egypt, several studies discussed the issue of coastal erosion along the Nile Delta coast based on beach and nearshore profiles semi-annually collected by stations belong to Coastal Research Institute (CORI) since the Eighties of the last century. Contemporary to that time the coastal research along the Nile Delta using remote sensing technology had been used (Klemas, and Abdel-Kader, 1982) and focused on mapping the shoreline and offers the potential updating maps in order to distinguish sites of erosion and accretion (Smith and Abdel-Kader, 1988) and led to subdivision of the coast into subcells of convergence and others of divergence waves (Frihy et al., 1991). In attempts to save beaches, such inadequate human intervention, led to an emergence of unsuccessful project enhanced the changes in morphodynamic. Consequently a new approach of thematic mapper imagery (El-Asmar and White, 1997) was used for the purpose of integrated coastal zone management along the Nile Delta using segmentation process, based on the orientation, the nature of shoreline sediments and the implemented defense measures. Later, Dewidar and Frihy (2010) estimated rates of shoreline changes from three statistical approaches of Digital Shoreline Analysis System (DSAS) (the end point rate, the Jackknife and a weighted linear regression) are validated with ground observations of beach profile survey data at the same positions. El-Asmar and Hereher (2011), Dewidar (2011) used two techniques to estimate rate of shoreline retreat. The first technique corresponds to the formation of automated shoreline positions by digitizing for mapping erosion/accretion pattern and the second one is for estimating rate of shoreline change based on data of remote sensing applying Digital Shoreline Analysis System (DSAS) software. The End Point Rate (EPR) was calculated by dividing the distance of shoreline movement by the time elapsed between the earliest and latest measurements at each transect. El-Asmar and Hereher (2011); El-Asmar et al. (2012, 2013), Hereher (2014) identified changes in lagoons surface area using water index algorithms.

The Damietta promontory as one of the two promontories of Nile river mouths at Damietta and Rosetta is a fragile costal area subjected to severe erosion, we emphasize on monitoring this coastal strip due to its economic and touristic value. This coast includes the elite, historical and favorable resort beach at Ras El-Bar. At present and due to population expansion, Ras El-Bar has become a new permanent community for about a quarter of million. Together, Ras El-Bar, the historical Damietta City with the Damietta Harbor and City represent the Damietta governorate of about 2 million of Egyptian populations, with tens of billions of EL investments in activities of real-estate, accommodations, hotels, and entertainments and the consequent taxes collected by the government related to such activities. In addition to shipping, logistics and free industrial zone at the Damietta Harbor and the traditional furniture industry at the Historical Damietta City, all these spots may be threatened by sinking hazards and complete disappearance of such activities.

1.1. The study area

The study coastal area at Ras El-Bar is part of this fragile Damietta promontory (Fig. 1A), which was described as wave convergent subcell (Frihy et al., 1991, 2003). At Ras El-Bar coast; several defense measures were implemented including two jetties lining the Damietta branch of the Nile River, seawall, revetment, three jetties and 8 detached breakers parallel to shoreline. Together these defense measures and the Damietta Harbor constructions led to the emergence of a new pattern of wave reflection with consequent erosion and accretion along the coast.

In the early 1980s, a decision was made to construct a new harbor and city to the northwest of Damietta (Fig. 1B) in order to increase the trade potential along the Mediterranean coast. It was also decided to construct the harbor some distance inland to be protected from winter storms so that it could be used year-round and avoid shipping delays. A site location (Fig. 1A) was selected in a coastal embayment with minimal effects from waves and currents (Sogreah, 1982). The selection of the harbor site is characterized by a wave divergent and a sediment convergent (sink area) (Abo Zed, 2007). Before the construction of the harbor (1978–1982), the coastal stretch extends from the Gamasa drain to the Damietta mouth (Damietta Harbor lies in the middle), it was marked by accretion (Abo Zed, 2007). The location was described by UNESCO/UNDP (1978) as one of long-term coastal accretion. It is supported by significant fields of active dunes fed by beach sands (Frihy et al., 1991; Fanos et al., 1995). The harbor (Fig. 1B) is composed of two parts: the shipping area, which is an inland basin containing 12 platforms, and an access channel connecting the shipping area with the Mediterranean Sea. In 1982, the entrance to the access channel was protected against littoral drift by two jetties, which were extended in 1985. The western jetty is 1300 m long and the eastern jetty is 600 m long (El-Asmar, 1995, Frihy et al., 2002). After the construction of Damietta Harbor (1988–1997), the western area of the harbor (2 km west) was marked by accretion, whereas the eastern area (5 km east) was marked by erosion (Fig. 4). This could be attributed to the fact that the western jetty (1.5 km long) interrupts the eastward sediment transport along the coast and blocks the eastern sediment transport. The annual net rate of littoral drift on the western side of the harbor is about 1.43 $\times$ 105 m^3 (accretion), while the annual net rate of littoral drift on the eastern side is about 2.54 $\times$ 105 m^3 (erosion) (Abo Zed, 2007). Presently, the Damietta Harbor is one of the Egyptian harbors expected to receive new investment projects such as the global logistics center for storage and handling of grain and cereals. The sustainable development of the harbor is a public request, and the most important hazards threatening the harbor are the erosion issue and siltation of the navigation channel. The latter was discussed in El-Asmar and White (2002); Frihy et al. (2002); Abo Zed (2007); and in Gad et al. (2013).

1.2. Wave climate

Wave action along the Nile Delta coast is seasonal with high storm waves approaching from the NW– NNW during the winter (October to March). These generate eastward longshore currents with velocities of up to 0.9 m s^{-1} (Tetra Tech, 1984), driving a sediment flux. Swells during the spring and summer are predominantly from NNW–WNW, with a small component from NNE (Fig. 2). These can cause either easterly or westerly sediment transport depending on local shoreline orientation (Fanos et al.,

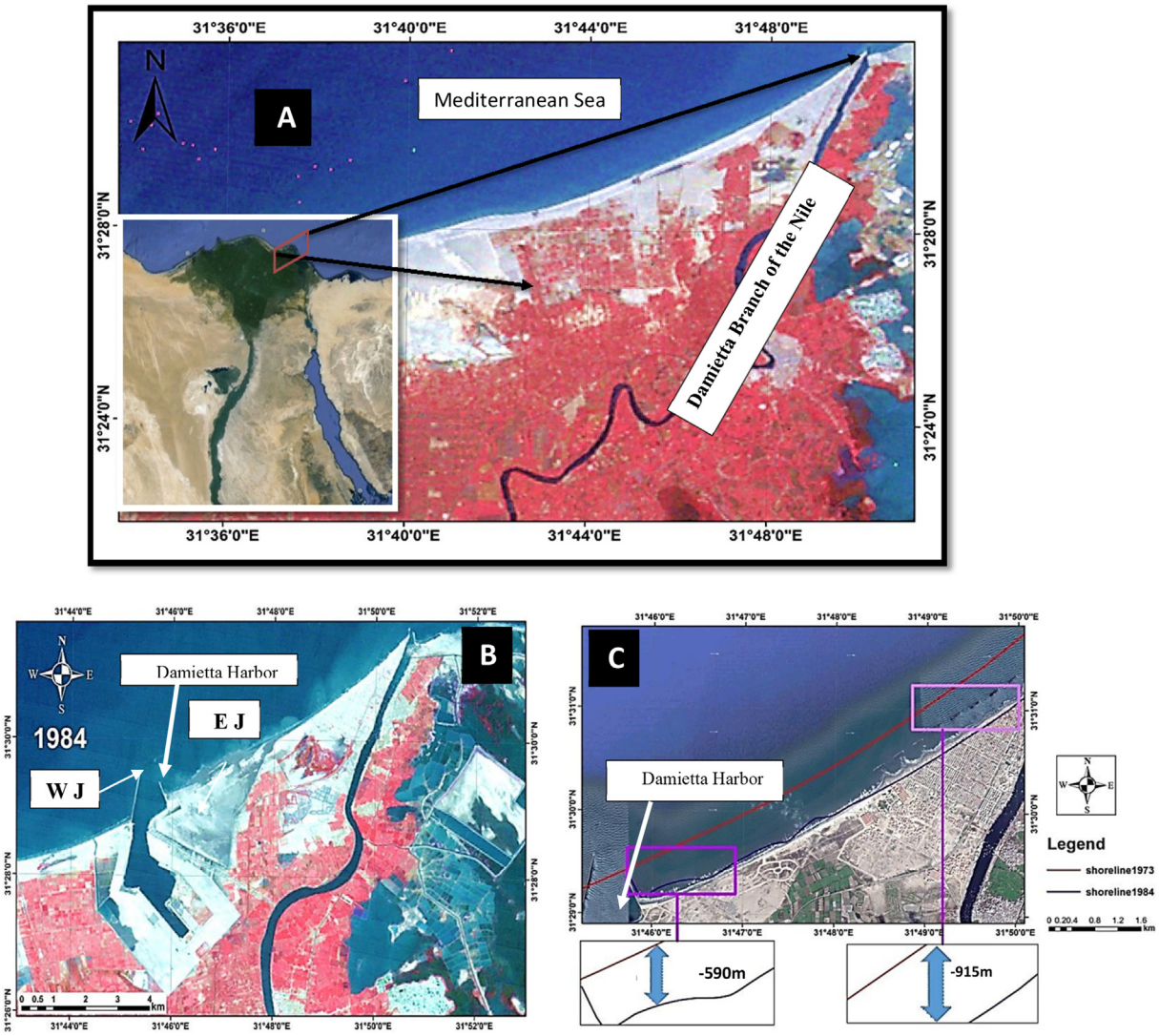

Fig. 1. (A) MMS Satellite image of 1973 showing the location of the study coast before excavation of Damietta Harbor, (B) 1984 after excavation of the harbor with two jetties protecting the navigation channel, the Western (WJ) and the Eastern (EJ), and (C) ETM Satellite image of Showing the main shoreline changes along Ras El-Bar coast from 1973 to 1984.

1995). Wave climatology data were collected from 1985 to 1990 at Abu-Quir, east of Alexandria, and Ras El-Bar, the modal significant wave height for both stations is 0.75 m and significant wave period is 7–8 s during winter decreasing to 5 s in summer (Frihy and Deabes, 2011). The Mediterranean Sea at the Nile Delta has an extremely low tidal range; measurements at the inlet to Lake Burullus show a mean tidal range (change in the level of the sea during one tidal day—approximately 25 h) of only 14 cm over the last 20 years (El-Fishawi, 1994), with 60-cm variation in daily mean sea level at Port Said over the period 1980–1986 (Eid et al., 1997). Several estimates of the magnitude of littoral drift have been made for this section of coast before the harbor was built. Sogreah (1982) estimates a drift of some 0.66 million $m^3\ yr^{-1}$ to the east and 0.26 million $m^3\ yr^{-1}$ to the west, resulting in a net annual transport of 0.4 million $m^3\ yr^{-1}$ to the east. Other estimates of net transport include $1.16 \times 10^6\ m^3\ yr^{-1}$, $0.8\ 10^6\ m^3\ yr^{-1}$ (Tetra Tech, 1984) and $0.6–1.8 \times 10^6\ m^3\ yr^{-1}$ (A.S.R.T, 1988).

1.3. Aims

The present study is part of our research program"Monitoring coastal changes along the Eastern Nile Delta" (El-Asmar, 1994; 1995, 2002; El-Asmar and White, 1997; White and El-Asmar, 1999; El-Asmar et al., 2014). The main objectives of this study are: (1) to monitor and update knowledge of this very dynamic and strategic segment of the coastline, (2) to determine its vulnerability to erosion problems related to hydrodynamic changes, (3) to introduce for the first time significant geomorphodynamic features emerged along this coasline due to the changes in beach morphodynamic as a result of human intervention. Such geomorphic changes were regionally detected using remote sensing application then land verification through field observations and photographing, and finally (4) to introduce our recommendations to the decision makers in order to secure the socio-economic community at the coastal zone of Damietta-Ras El-Bar.

2. Methods, data and processing

Remote sensing techniques are considered among the best solutions for detecting the regional changes and exploring the new phenomena over the earth surface. Satellite remote sensing has proved its utility in all fields of earth sciences including the study of

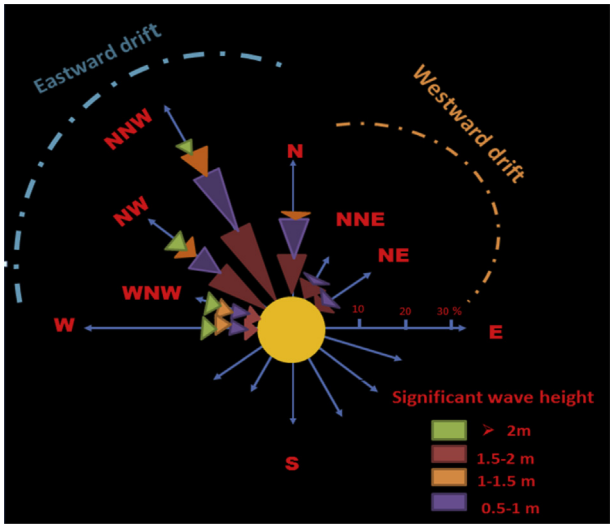

Fig. 2. Directional distribution of significant wave heights showing the predominant winter wave approaching from the NNW, NW, and WNW is responsible for generating the eastward longshore drift the opposing summer waves occasionally approach from the NNW, N, NNE and NE sectors.

changes in the coastal processes and morphology (Guneroglu, 2015), and the assessment of shoreline movement because of the repetitive, synoptic and multispectral coverage's of the satellites (Alesheikh et al., 2007; Rao et al., 2009). It has also the potential to provide accurate and time-wisely geospatial information describing changes in land use/land cover (LU/LC) (Foody, 2003; Herold et al., 2002; Yuan et al., 2005; Guneroglu, 2015). On the other hand, multispectral remote sensing satellites provide digital imagery in various spectral bands, including the near infrared where the land-water interface is well defined. Furthermore, this approach has several advantages; it is not time consuming, inexpensive to implement, large ground coverage, and has the capability for repeat data acquisition and monitoring (Van and Binh, 2008).

Generally, change detection involves the application of multitemporal data sets to quantitative analysis of temporal change of the phenomenon (Lu et al., 2004; Srivastava et al., 2012). The basic principle behind using digital data is that any subtle change in LU/LC results in a change in the radiance of that object detected by satellite sensors (Mass, 1999) at a range of spatial, spectral and radiometric resolutions. For example, the conversion of land use from rural to urban land causes change in the visible portion of the spectrum (brightness). The change from vegetation to non-vegetation land use causes difference in the near-infrared (NIR) radiation (greenness), and the change in the shortwave-infrared (SWIR) reflects change in moisture content (wetness) (Lunetta and Elvidge, 1998; Lu et al., 2004). LU/LC change detection generally employs one of two basic methods: pixel-to-pixel comparison and post-classification comparison (Dennis and Colfer, 2006, Dewidar, 2004; Mukherjee et al., 2009), which compares two or more separately classified images of different dates (Serra et al., 2003; Shalaby and Tateishi, 2007). Post classification comparison is considered the more appropriate and commonly used method for change detection (Lillesand et al., 2004).

Landsat images data covering the study area have been digitally processed, analyzed and interpreted to produce a LU/LC map at a scale of 1: 50.000. This is based mainly on the multilevel LU/LC classification system used with remote sensor data adopted by the U.S. Geological survey (Anderson et al., 1976). The produced Landsat image classification map clearly displays the major classes of LU/LC. This necessitates the use of geometric rectification algorithms that register the images to each other or to a standard map projection. In addition, most of the methods require a decision as where to place the threshold boundaries in order to separate areas of change from those of non-changes.

Change detection is the use of remotely sensed imagery of a single region, acquired on at least two dates, to identify changes that might have occurred in the interval between the two dates. The calculated average shoreline changes and the total area for identified segments in regions showing significant variations are something very critical as the shoreline is a dynamic and complex, it has mixed results of tidal, aeolian, tectonic, and sometimes riverine. The shoreline change has its impact, but it is not so visible, to observe this we need a long and continuous set of data. In the present study a shoreline length of approximately 9.9 km was examined, and a series of image data are acquired at unequal intervals between 1973 and 2015, that is, covering a time span of 42 years (Table 1). These series includes five shorelines: 1973, 1984, 1998, 2003, and 2015. The data acquired from the GLOVIS and EARTH EXPLORER sites, maintained by USGS. The study area is covered by the Thematic Mapper (TM) and Enhanced Thematic Mapper (ETM+) scene (Path/Row 176/38), and by (Path/Row 189/38) for the multi-spectral scanner (MSS). All image scenes are subjected to image processing using ENVI software version 5.1. The selected based on the criteria of Cloud cover less than 10%.

The method of processing of the satellite images (Fig. 3A) started with the geometric correction was performed through image-to-image geo-referencing in the Universal Transverse Mercator Projection (UTM/zone 36 WGS 84) using a first-order polynomial transform. At least 20 prominent well-distributed ground control points (GCP) selected in the master images, located in the other images, and then a nearest neighbor resampling method was applied. (El-Asmar et al., 2013; Jayson-Quashigah, 2013; Hereher, 2014; Deepika et al., 2014). All the optical images, after geometric and radiometric corrections, were then digitally processed using the Water Index method. The Water Index is one of the band ratios where the sum of visible bands is divided by the sum of the infrared bands (Braud and Feng, 1998; Mahboob and Atif, 2016). The procedure aims at obtaining the sharp edge between water and land as water reflectance is more pronounced in visible bands, while absorption is dominant in the infrared band. Using this characteristic, this technique was applied on the images and threshold level slicing was done to distinctly separate landmass from the water. The sharp edge between the two classes refers to the shoreline. Then in the GIS environment the sharp shorelines were digitized (Thieler et al., 2005), and the layers of multi date shorelines were prepared for 1973, 1984, 2003, 1998, and 2015 in the line feature class. Using the overlaying operations and spatial analyst tools the analysis for spatial and temporal change detection had been done. To study the spatial change pattern along the shoreline, cross sections (Fig. 3B) were taken almost at the 90° angle across all the shorelines, digitized and amount of the shift of the shorelines in a certain time-interval were measured. It gives the spatial shift of the shoreline over the time. Then cells were generated over the total amount of shifts. (Santra Mitra et al., 2013; Ozturk and Sesli, 2015). Because the images being acquired in different seasons, it was crucial to make an atmospheric correction and radiometric normalization to all images in order to get comparable data at the same level (Chander et al., 2009; Tyagi and Bhosle, 2011) and eliminate effects of dust, haze and smoke as well as the solar angle variations. Atmospheric correction was carried out to all images by subtracting the minimum pixel value from the pixel matrix of each image (dark object subtraction) (Chavez, 1996). The dark object was chosen to represent the clear deep water of the Mediterranean Sea. As the solar angles are different in all images, it was crucial to

Table 1
Satellite data acquired and utilized in the present study in a chronological order from 1973 to 2015.

Satellite	Sensors	Spectral bands (lm)	Resolution (m)	Date	Path/row
Landsat4	MSS	0.5–0.6 visible green 0.6–0.7 visible red 0.7–0.8 near infrared 0.8–1.1 infrared	60	23-0ctober-1973	189/38
Landsat5	TM	0.45–0.52, visible blue 0.52–0.60, visible green 0.63–0.69, visible red 0.76–0.90, near infrared 1.55–1.75, infrared 10.4–12.5, thermal 2.08–2.35, infrared	30	20-September-1984	176/38
Landsat5	TM	0.45–0.52, visible blue 0.52–0.60, visible green 0.63–0.69, visible red 0.76–0.90, near infrared 1.55–1.75, infrared 10.4–12.5, thermal 2.08–2.35, infrared	30	7-Jun-1998	176/38
Landsat 7	ETM	0.45–0.51, visible blue 0.53–0.59, visible green 0.63–0.69, visible red 0.78–0.90, near infrared 1.55–1.75, infrared 10.4–12.5, thermal 2.09–2.35, infrared 0.52–0.90, panchromatic	30	3-August-2003	176/38
Landsat8	OLI	0.43–0.45 coastal 0.45–0.51 visible blue 0.53–0.59 visible green 0.63–0.67 visible red 0.85–0.87 near infrared 1.56–1.65 infrared 10.6–11.1 thermal 11.5–12.5 thermal 2.10–2.294 infrared 0.503–0.676 panchromatic 1.363–1.384 cirrus	30	19-April 2015	176/38

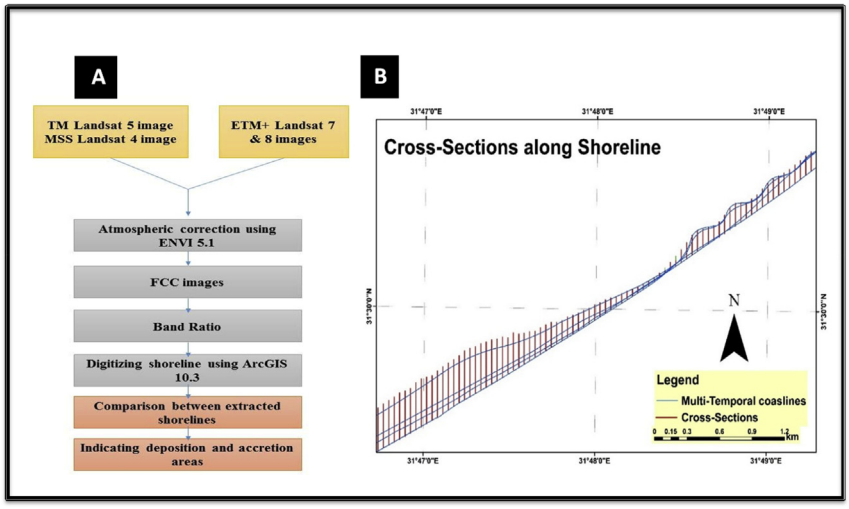

Fig. 3. (A) Flow chart showing the applied procedures on the selected satellite images for the present study, (B) and cross-section showing how we calculate shoreline changes based on right angles on the base shoreline of 1984.

normalize these angle variations as they were subjected to radiometric normalization taking into account the earth–sun distance, the solar elevation angle, and the dark object (minimum pixel digital number). The radiometric correction was applied using the COST Model in ERDAS Imagine producing normalized images of reflectance values and ready for subsequent processing.

For visual interpretation of the data a False Color Composite (FCC), which is a combination of IR, Red and Green positioned in R, G, B respectively is used. This is because the data we are using has a low resolution. So every pixel indicates an average value of a large area. The True Color Composite of RGB may be inefficient in such situations. But the use of FCC greatly improves our understanding

of various features in a data bodies (Lillesand and Kiefer, 1994). The data acquired were of individual bands, so the bands required for the FCC were added and the FCC was created in ENVI software version 5.1.

3. Results

3.1. Remote sensing applications

As mentioned before the site of the Damietta Harbor was selected in a coastal embayment with minimal effects of waves and currents. It was described as one of long-term coastal accretion at a divergent subcell. However, comparison of the satellite images of (1973) before and (1984) after the construction of the Damietta Harbor reveals the presence of coastal erosion with shoreline retreat along the whole coast between the Damietta Harbor and Ras El-Bar (Fig. 1C), totally being −590 m and increased eastward to the Damietta promontory to reach −915 m, with an average of −53.6 myr^{-1} and −83.2 myr^{-1} respectively. During this period no obvious shoreline changes is detected to be related to the human intervention. The shoreline changes in concern is that contemporaneous to the construction of two entrance jetties along the Damietta Harbor, which led to emergence of a new wave and current pattern with up drift deposition and down drift erosion to the west and east of the harbor respectively (Fig. 4A and B).

Measurements for shoreline changes have been taken at 9 stations along the coast between the Damietta Harbor and Ras El-Bar (Fig. 4B). They reflect two coastal segments (Fig. 5A, and Table 2). The eastern segment shows accretion at the shadow of detached breakwaters, with a gained area of 0.46 km^2 and shoreline advance of 3.54myr^{-1} (Fig. 5A). On the other hand, the western segment, which is located between the western tip of the detached breakwaters at Ras El-Bar and the eastern jetty of the Damietta Harbor, is suffering from erosion and shoreline retreats. The eroded area at the western segment reached 0.57 km^2 with an average shoreline retreat of −7.14 m yr^{-1}. The retreat along the shoreline from 1984 to 1989 (Fig. 5B) was −7.43 myr^{-1}, then increased from 1998 to 2003 (Fig. 6A) to reach −10.90 myr^{-1}, and again decreased after the extension of the detached breakwaters from 2003 to 2015 (Fig. 6B) to −3.11 m yr^{-1} (Table 2). The longshore transport pattern along the western erosional segment at the down drift of the eastern jetty of the Damietta Harbor reflects an upward increasing rate with a maximum of 449 × 10^3 m^3 yr^{-1}, and continuous erosion (Frihy et al., 2003) except during the period from. 1984 to 1987 an accretion equal to 304 m was observed, which interpreted by El-Asmar et al. (2014) as related to disposal of more than

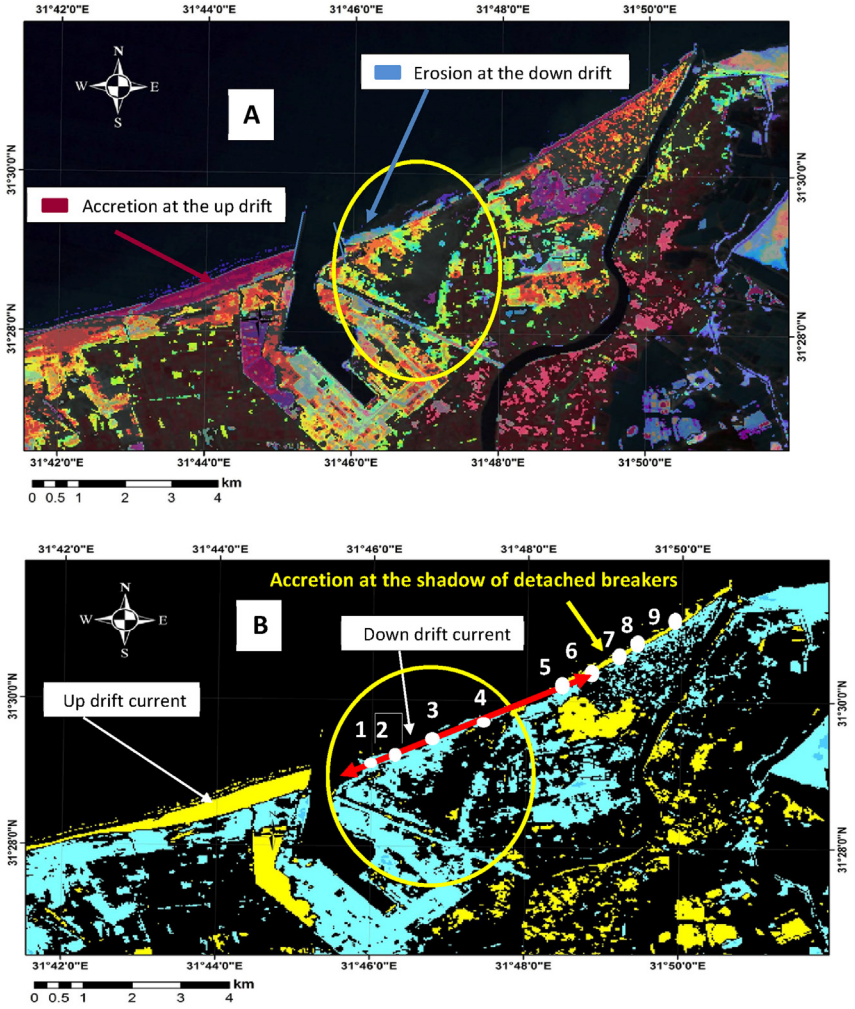

Fig. 4. (A) ETM Satellite image showing change detection between 1984 and 2015 with shoreline accretion at the updrift of the harbor western jetty and erosion at the down drift of the eastern jetty, and (B) both positive (yellow) and negative (blue) changes along the shoreline. The yellow circle at both photos shows the position of sediments dredged through the excavation of the navigation channel. The white points from 1 to 9 refer to the stations selected for measurements of shoreline position and beach profiles along with the baseline (red line). (For interpretation of the references to colour in this figure legend, the reader is referred to the web version of this article.)

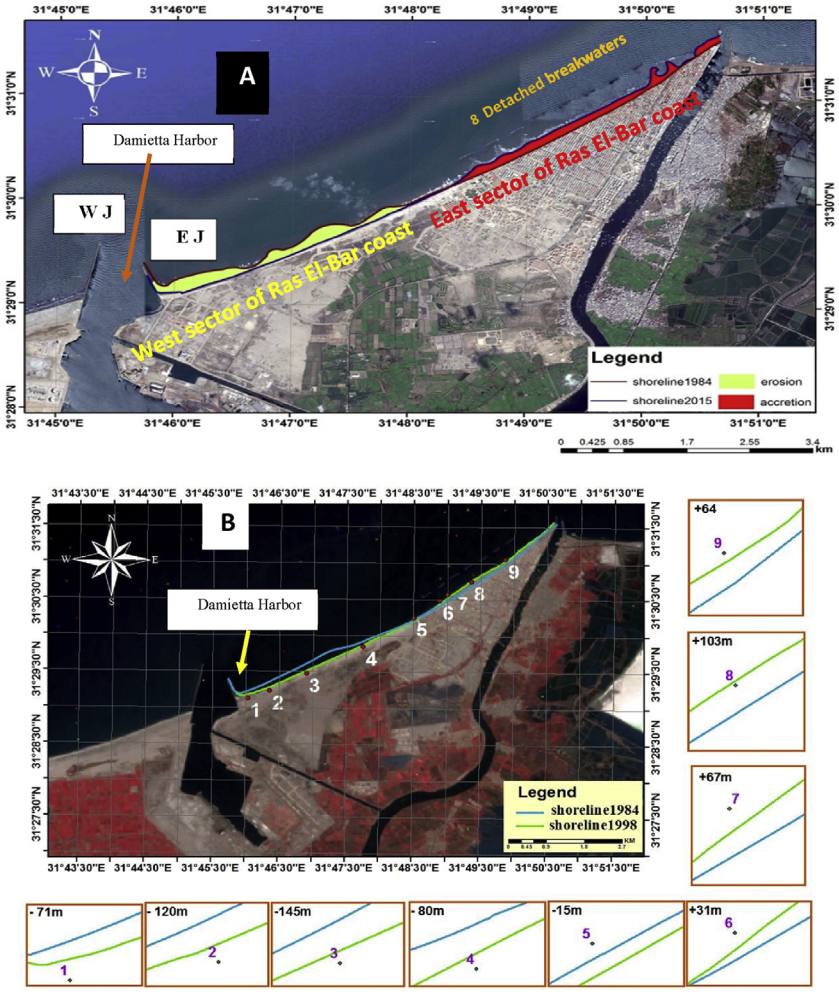

Fig. 5. (A) Segments subdivision of the studied coast into eastern accretional one (red) and western erosion one (yellow), and (B) detection of the shoreline position for the period from 1984 to 1998. (For interpretation of the references to colour in this figure legend, the reader is referred to the web version of this article.)

Table 2
Changes in shoreline across the studied two segments and transitional point 5 at the end of detached breakers. During the periods 1973–1984, 1984–1998, 1998–2003, and 2003–2015.

The present study												
Stations	Segments	1973–1984		1984–1998			1998–2003			2003–2015		
		11 yrs.	m/yr.	14 yrs.	m/yr.	Average	5yrs.	m/yr.	Average	12 yrs.	m/yr.	Average
1	Western Segment	−590	−53.6	−71.00	−5.07	−7.43	−85.00	−17.00	−10.90	−30.00	−2.50	−3.11
2				−120.00	−8.57		−50.00	−10.00		−45.00	−3.70	
3				−145.00	−10.36		−47.00	−9.40		−60.00	−5.00	
4				−80.00	−5.71		−36.00	−7.20		−15.00	−1.25	
5	End of break water system			−15.00	−1.07		+28.00	+5.60		+10.00	+0.83	
A				−16.00	−1.14		+9.50	+1.90		−4.50	−0.38	
B				−19.00	−1.30		+16.50	+3.30		+1.50	+0.16	
6	Eastern Segment	−915	−83.2	+31.00	+2.21	+4.73	+48.00	+9.60	+5.00	+3.50	+0.29	+0.89
7				+67.00	+4.79		+50.00	+10.00		+24.00	+2.00	
8				+103.00	+7.36		−20.00	−4.00		+6.00	+0.50	
9				+64.00	+4.57		+22.00	+4.40		+9.00	+0.75	

5×10^6 m^3) of sediment dredged during the excavation of the harbor entrance and navigation channel (Frihy et al., 1991; El-Asmar, 1995), such dredged sediments have been stored along the eastern down drift coast (Fig. 4).

At station 5, three points 5, A, and B at the end of the detached breakers (Fig. 7A and B) showed erosion from 1984 to 1998, with averages shoreline retreat of −1.07 m, −1.14 m and −1.30 m yr^{-1} respectively. These values seem in accordance with the whole western segment at the same periods (Table 2). After complete construction of detached breakwaters (totally 8 detached breakers) the pattern in 1998–2003 was reversed with accretion at the points 5, A, and B and shoreline advances being +5.6 m + 1.9 m, and+3.3 m yr^{-1} respectively. From 2003 to 2015 at the western tip of breakwater 8, the accretion decreases at the two points 5, and B

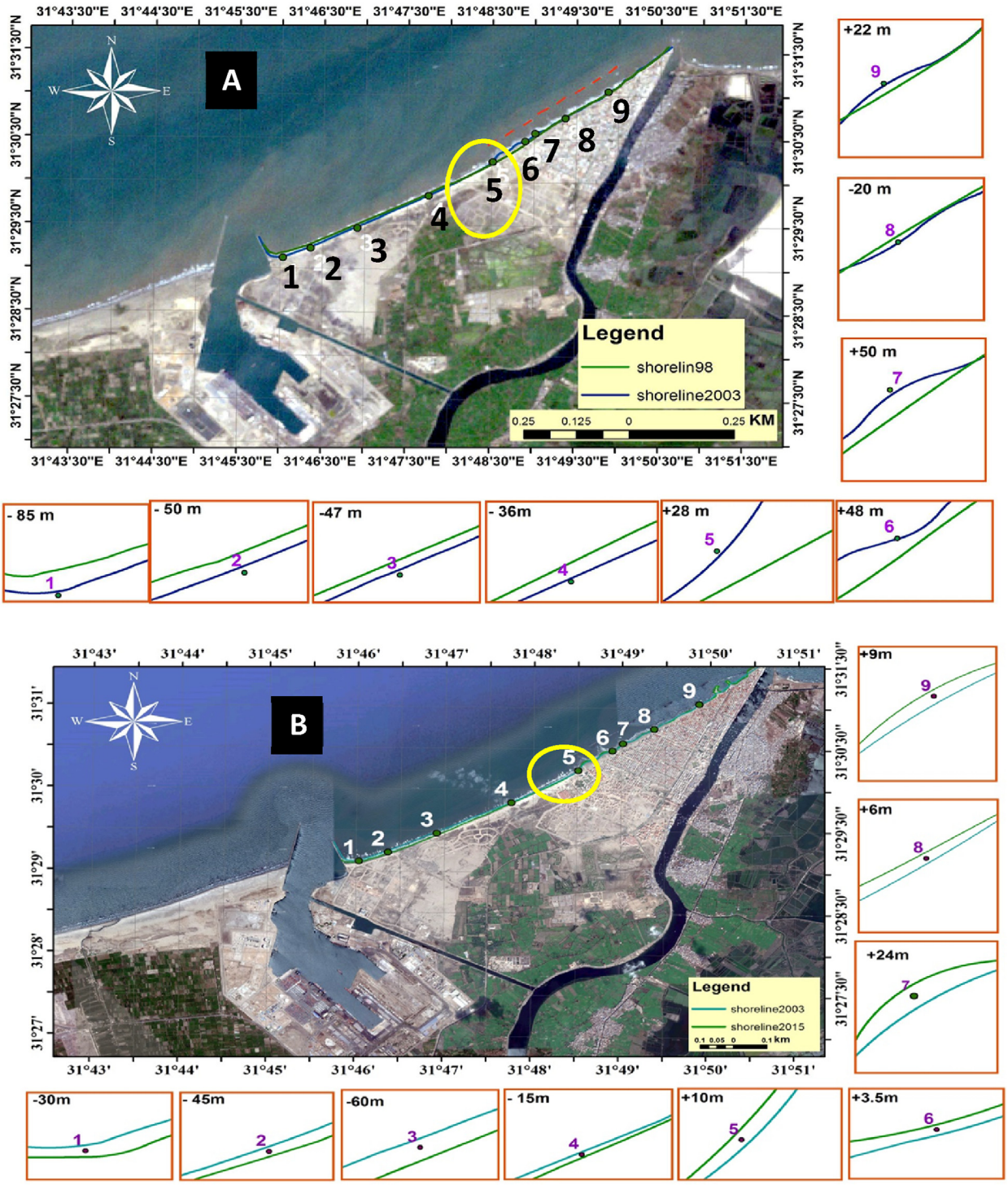

Fig. 6. (A) ETM Satellite images showing shoreline changes between 1989 and 2003, and (B) between 2003 and 2015. The yellow circles in both photos A, B refer to the eroded embayment at point 5 closely shown in Fig. 7. (For interpretation of the references to colour in this figure legend, the reader is referred to the web version of this article.)

being +0.83 m, and +0.16 m yr^{-1} respectively, with noticeable erosion (−0.38 m) at point A (Fig. 6, and Table 2). Similar erosion was observed at the up drift of the detached breakwaters, in 1994 when they were only four of them, and interpreted as related to the development of an adverse eddy waves resulted due to collision of strong waves outside the breakwaters area with the stagnant waves ~) 25%) at the shadow area of the detached breakers (El-Asmar, 1994). Such eddies appeared again at the up drift tip when the detached four breakers became and led to the development of erosional embayment at point 5A (Fig. 7A–C).

3.2. Beach profiles

A detailed survey of the foreshore-backshore zone is carried out using a theodolite and six profiles measured from baseline at five points located along the studied coast (Figs. 4B and 8).

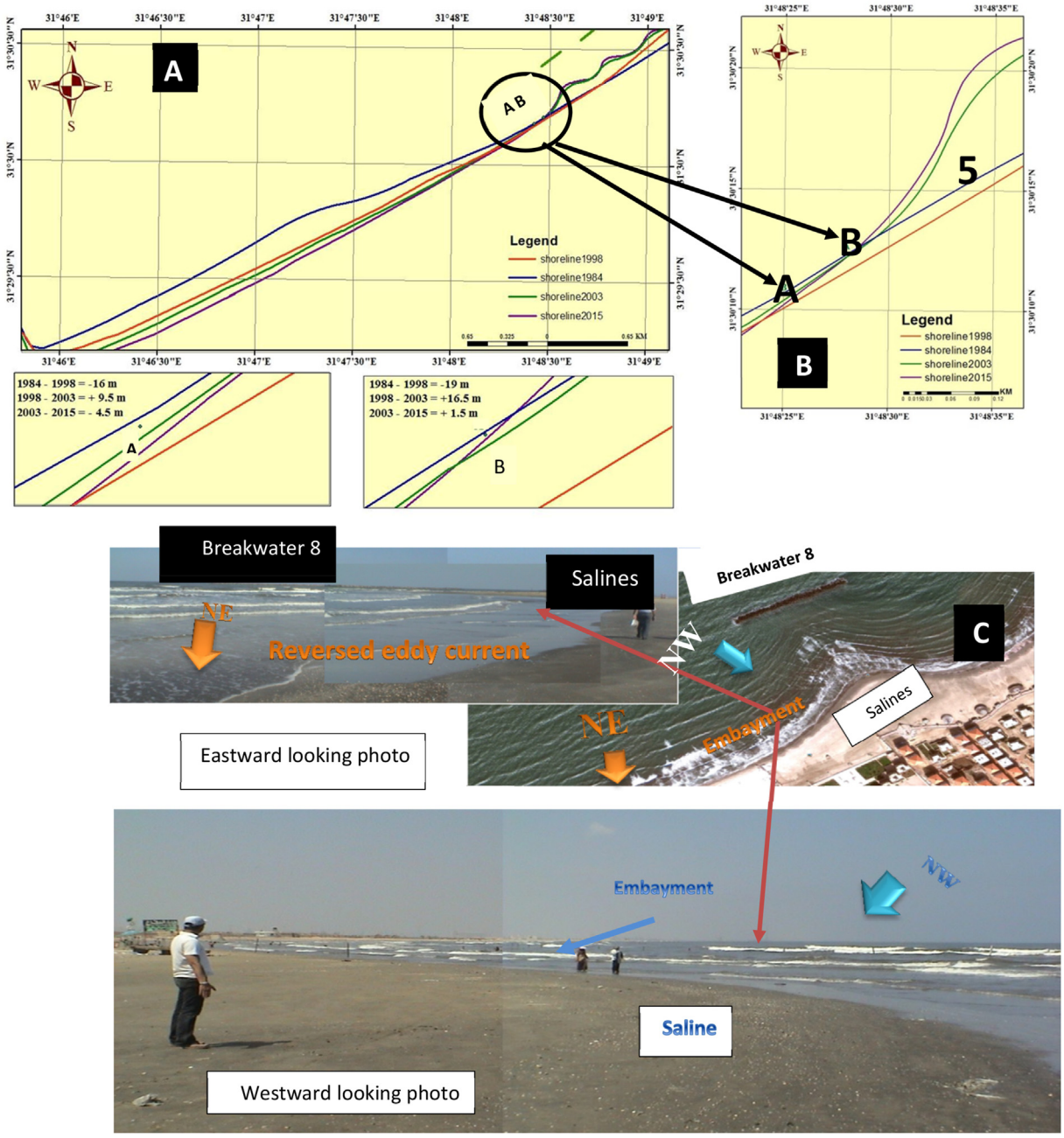

Fig. 7. (A, B) Closeup showing the western erosional coastal segment with detailed shoreline changes from 1984, 1998, 2003 to 2015. (C) Field photo showing the embayment formed at the end of detached breakers at point 5 of Figs. (6, 7B).

The stations from 1 to 4 selected to represent the erosional coastal segment (Figs. 4B and 8 from 1 to 4). The fifth station has taken as an example for the accretional points at the shadow area of the detached breakwater no.8 (Fig. 7B points 5, A, B, Fig. 8-5, 5B). The profiles measurements are plotted on a regression diagram and illustrated in Fig. 8. The erosional segment show steep slope profiles with averages of 1/4.4, 1/6.9, 1/6.7, and 1/5.0 for the stations from 1 to 4 respectively. At station 5 two profiles 5A and 5B (Fig. 8) have been measured, the first at point 5A is erosional with a steep slope 1/4.6 located in the embayment at the end of detached breakers no.8 (Fig. 7A–C, point A, and Fig. 8-5A). The second is accretional, gently sloped beach with an average of 1/19 (Fig. 7A–C, point B, Fig. 8-5B, 10G). During our field observations the steepest scarp developed in the western erosional segment (Fig. 9E and 10A). A new revetment project (Fig. 9A and B) was installed at the stations from 1 to 3 (Fig. 4), it is 1.5 m height composed of loose carbonate blocks, and constructed in two parts, the first is a 320 m length, and the second is a 640 m length. This made to support the eastern jetty of the Damietta Harbor and to protect an area supposed to have a big heavy industry of nitrogen fertilizers by Agrium Company (Fig. 9A and B). However, the revetment partially collapsed due to sand dredged by waves and drifted by longshore current.

3.3. Beach type and swash beach cusps

Some morphologic aspects are observed and easily used to distinguish the coastal segments, of which are the rhythmic, nearly

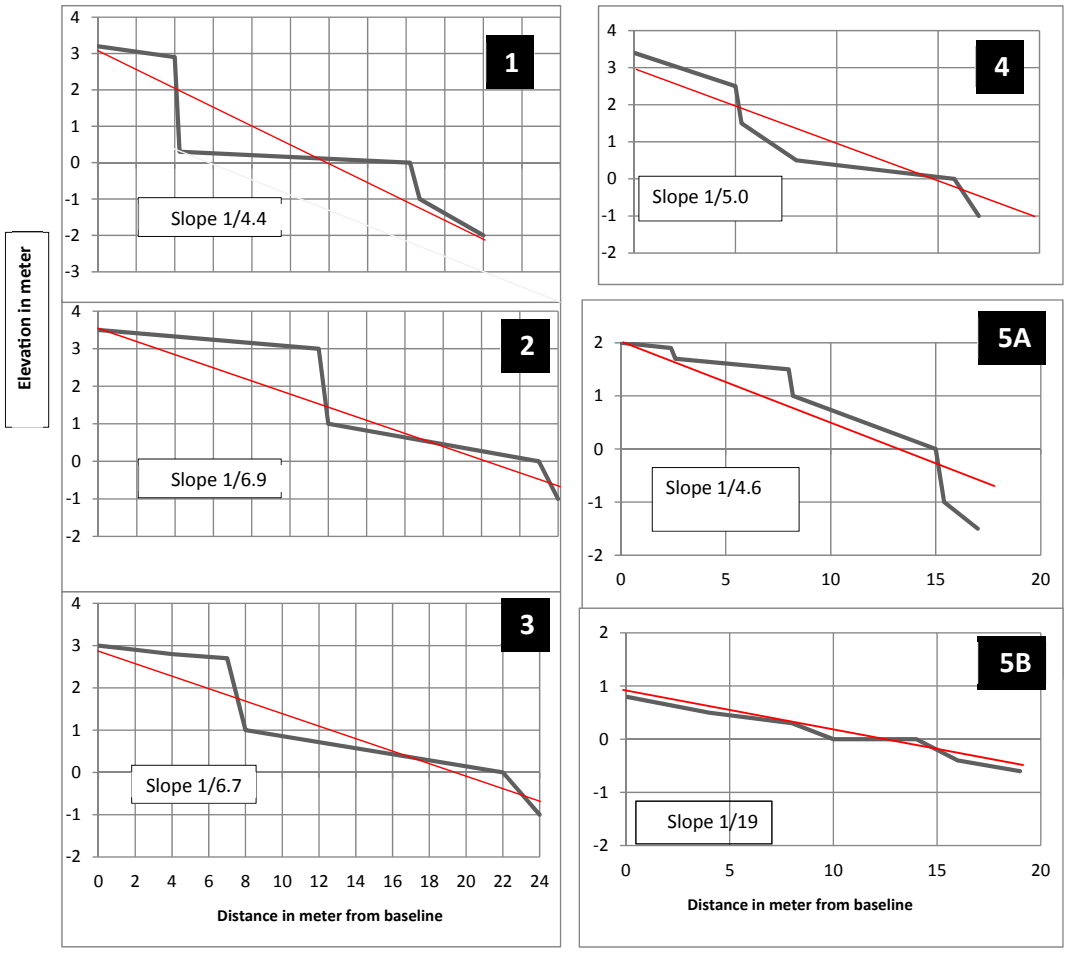

Fig. 8. The beach profiles with average slopes along the selected stations for the study area. The profiles from 1 to 5B represent the erosional beach while 5 selected to represent the accretional beach at the shadows of the detached breakwaters at No. 8 at Fig. (7C).

equal sized and spacing foreshore topographic features known as beach cusps, making crescentic shoreline formations, concave seaward, that are characterized by uniform longshore wavelength or spacing between horns (Komar, 1971, 1975; Holland and Holman, 1996; Lopes et al., 2011). Cuspate beaches normally associated with erosional processes (Asbury and Sallenger, 1979; Inman and Guza, 1982). Cusps appear to develop when waves are parallel to shore, approaching it at a 90° angle, but they may also form when waves approach at an oblique angle (Thornton et al., 2007).

In the present study, swash cusps are ranging from 6 to 15 m and associated with the reversed rip currents (Fig. 9 C, D, and E). The cusps not only observed at the beach but leave imprints on the erosional muddy scarp (Fig. 9E). Thornton et al. (2007) confirmed the association of swash cusps with rip currents, both are features (Fig. 9C and D) associated with the intermediate - reflective beach (Wright and Short, 1984; Komar, 1998; Lorang et al., 1993; Miles and Russell, 2004; Aagaard et al., 2012, 2013), with the characteristic steep slope, storm or winter profile, and plunging or surging wave breakings on the beach or collapsing over the step (e.g. Wright et al., 1979, 1982; Masselink et al., 1997; Masselink and Pattiaratchi, 1998; and Coco et al., 2000).

3.4. Plunging breakers and shelly beaches

As most of the dominant waves affecting the study area are long waves (H 0.5–1 m and T 6.5s, Frihy et al., 2003), a conditions suitable for plunging breakings occur when the sea floor is steep (Fig. 10 A) or has sudden depth changes and low tidal range (Dean and Dalrymple, 1991; Arkhipenko et al., 2002), with generation of clear step below the sea water level (Chanson and Lee, 1997; Short, 2012; Pedrozo-Acuña et al., 2010, 2011; 2012). Coco et al. (1999) reported evidence for a plunging breaking type being associated with the presence of cusps, and the development of a plunge step (King, 1972; Shepard, 1973; Davis, 1985). Due to its high energy, sediments along this step are typically coarse grained with concentrations of shell debris (Davis, 1985). On the other hand, “shell beach” is defined as a sea beach that routinely has an unusually large accumulation of sea shells washed up on it. Sea shells are most often the dead empty shells of marine mollusks. As the beach become steepness, the plunge step moves shoreward and most of its shell materials pushed away to the beach forming a shell beach The occurrence of beaches composed predominantly of shells and shell material provides evidence of converging waves associated with a steep slope (Watson, 1971). In the present study, shell beach (Fig. 10E and F) occurs on the western segment of the coast, where both the berm and beach face are steep (Fig. 10E). Most of detected shells belong to bivalves and some gastropods (Figs. 11 and 12, and Table 3).

4. Discussion

The results emerged for shoreline changes along the coastal

Fig. 9. (A) 1.5 m height carbonate revetment in two parts, the 1st 320 m length started eastward from the Eastern Jetty of Damietta Harbor, and the 2nd 640 m length with 4 m apart along the coast. (B) Close up of the revetment showing how much it is composed of loose blocks randomly arranged and partially collapsed. (C) Satellite image, showing the beach cusps and rip current, with reworked mud clasts. (E) Field photo for the beach cusps, rip current, with low tidal bars and crescentic troughs (D). The eroded muddy cliff with 3 m height and the crescentic edge reflect the wave effect on the cuspate beach.

zone between Ras El-Bar and the Damietta Harbor using remote sensing application reveal subdivision of the coast into two segments; the eastern and the western ones. The field verifications of both segments together with beach profile measurements reveal distinguished geomorphodynamic changes along those two segments. The eastern segment, developed at the shadow area of the detached breakwater system. It is an accretional one with total deposition of an area equal to 0.46 km^2 (Fig. 5A), during the period form 1984–2015 with an average shoreline advance of 3.54myr^{-1}. It is characterized by gentle slope beach face of 1/19 (Fig. 8, profile 5B, and Fig. 10G). The western segment shows evidence of coastal erosion with total loss of the coastal area equal to 0.57 km^2 during the period from 1984 to 2015 (Fig. 5A), with an average shoreline retreat of −7.14myr^{-1}. It is characterized by a steep slope beach face with an average slope of 1/5.72. (Fig. 8 profiles 1–4). The Nile Delta beaches were described as fully dissipative, fully divergent smooth wide beach face, gentle sloping, composed of fine to very fine sand and exhibit a very low-gradient (tan 3 = 0.05 to 0.02.; Nafaa and Frihy, 1993). Due to sea level rise and human intervention, the Nile Delta coast is no longer a dissipative or divergent one, and new patterns of waves and currents have resulted in new beach segmentations in response to the shoreline direction, the relation to induced waves and currents, and the implemented defense measures.

In the study area, the western segment shows some geomorphic features including cuspate beach, rip currents (Fig. 9 C, D), scarps (Figs. 9E and 10 A) and shell accumulations (Fig. 10E and F). The cuspate steep slope beach face (Fig. 9 C, D, and E), with medium to coarse grained clean sand (Fig. 10E) and shoreline retreat with a convergent waves, indicate features of intermediate state “d”

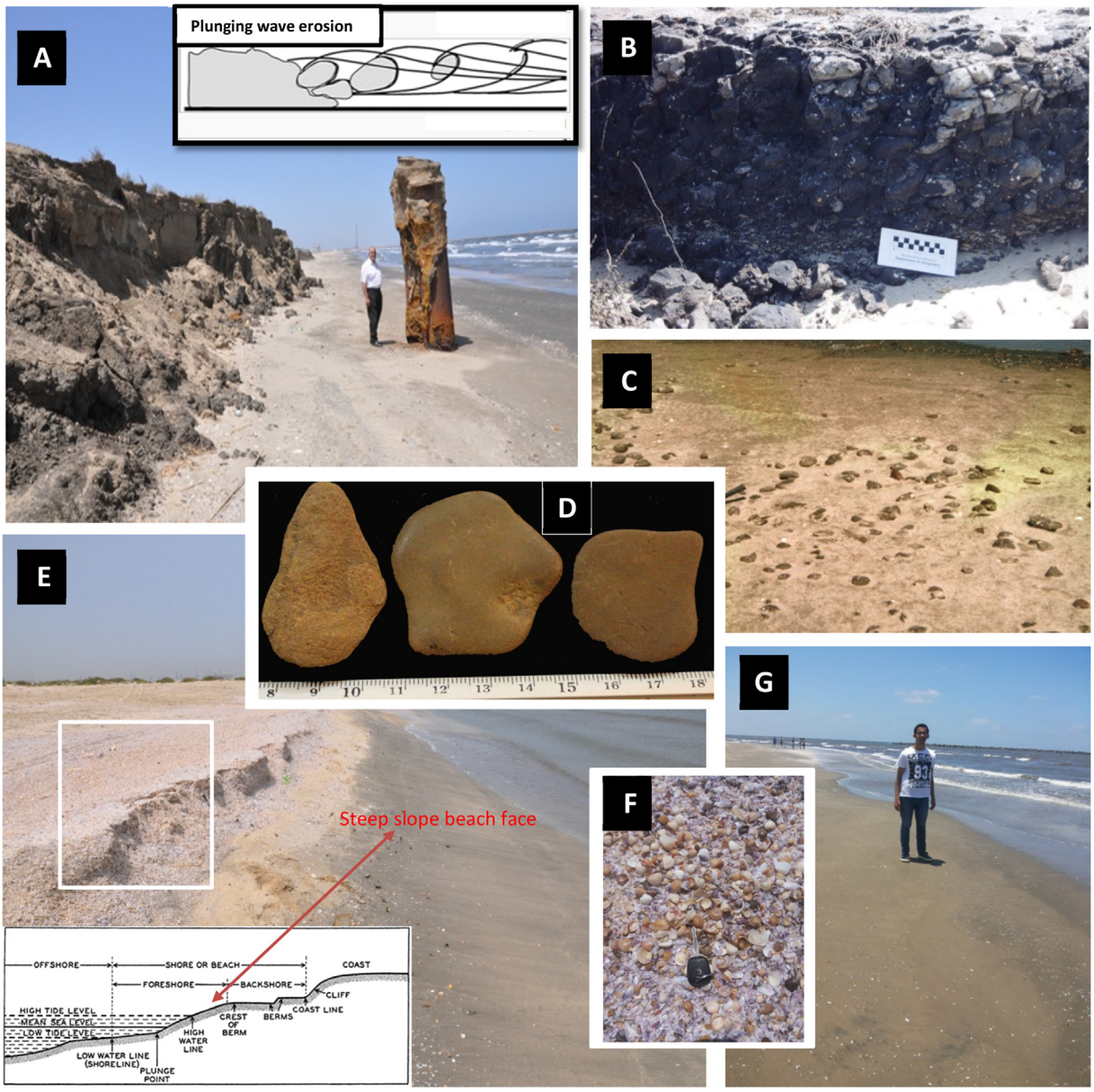

Fig. 10. (A) The muddy cliff of 3 m height, formed due to the plunging wave mechanism. (B) The mud clasts are eroded from the cliff, and (C) reworked at the beach eventually (D) forming discoidal platy gravels. (E) The reflective, eroded shelly beach with steep slope berm and beach face with foreshore profile showing plunge step where most by valves accumulated and thrown shoreward during storms and (F) close up showing thick shell accumulation. (G) The dissipative, accretional, low gradient beach composed of fine black sediments with lack of shell accumulation.

described in Wright and Short (1984) or intermediate reflective. On the other hand, the eastern segment, at the shadow of the detached breakwaters, the beach is accretional, gently sloped, fine grained relatively dark sands enriched with mud and heavy minerals, and spilling wave breaks, features characteristic for the dissipative divergent beach (Komar, 1998). At the western segment of the present study, the plunging breaking waves are responsible on severe coastal erosion and formation of scarp of about 3 m height (Fig. 10A). Such escarpment was excavated through the muddy sediments, which dredged from the navigation channel and stored to the east of the Damietta Harbor (Fig. 4). The plunging waves break down the coherent sediments, dragged and rolled along the beach forming the mud clasts (Fig. 10B and C). The latter eventually transformed into gravel sized discoidal mud (Fig. 10D). Similar mud clasts observed along the coast Northeastern Red Sea, South Al-Wajh, Saudi Arabia and interpreted as related to erosion and reworking by wave action (Ghandour et al., 2013).

The occurrence of shell accumulation, together with evidence of plunging breaking, occurrence of cusps and rip currents in a convergence waves, confirm the idea of the presence of adverse eddy waves generated at the upward current of the detached breakwater system (El-Asmar, 1994, 1995), such eddy waves have recently been recognized by El-Banna and Hassaneen (2002). Furthermore, they admitted the responsibility of eddies for drowning of average of 70 victims/year (El-Banna, 2006). Such eddies are responsible on convergence of waves that creates erosion, steepness and shell accumulations. The plunge step (Fig. 10E) is known to the rural oystermen as the 1st island, where empty dead shells are accumulated, and locally known as “Kishr”. Usually, local oystermen used to collect shells during winter, when

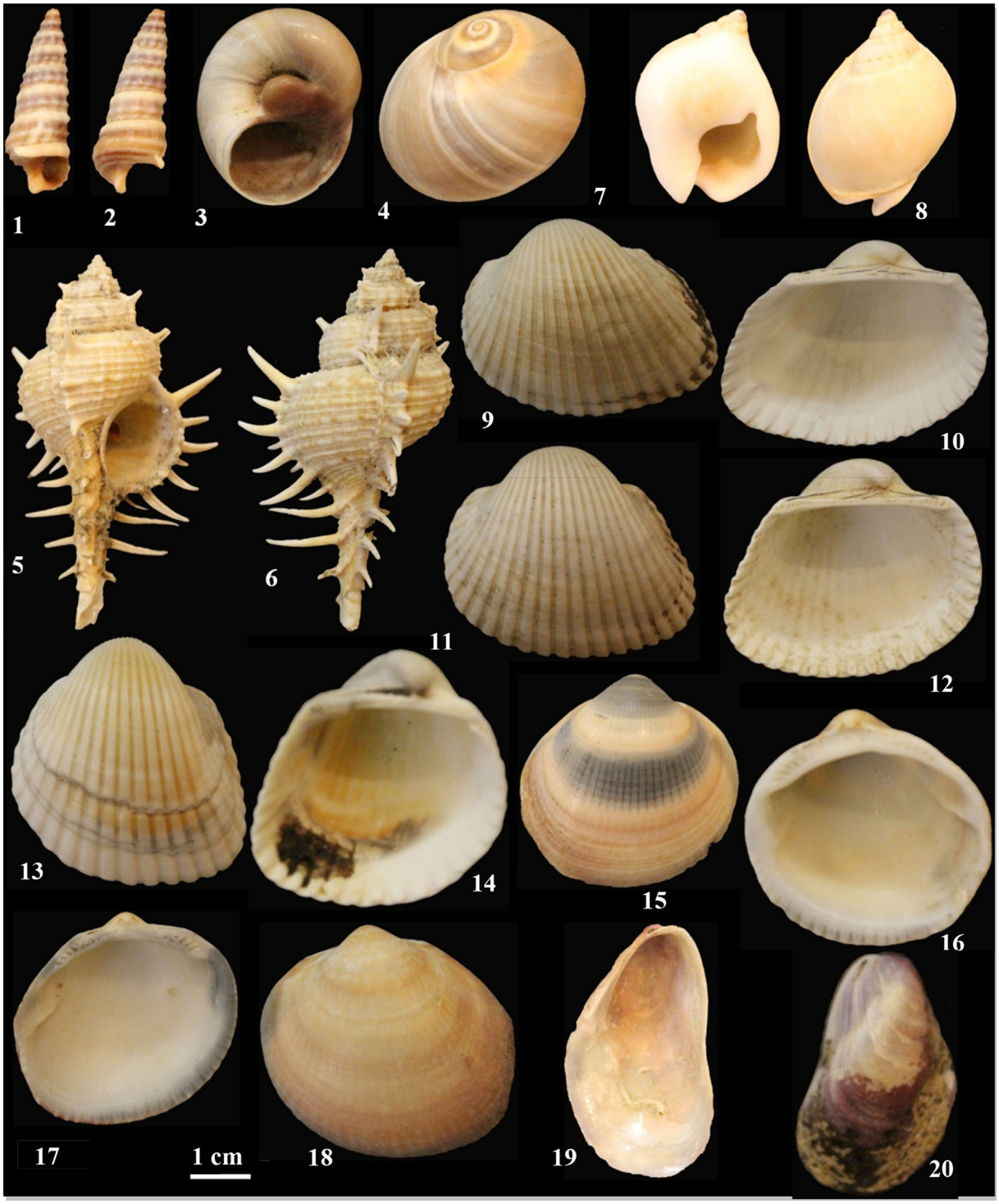

Fig. 11. 1, 2 *Cerithidea cingulata* (Gmelin, l79l). 3, 4, *Neverita (Glossaulax) didyma* (RÖding, 1798). 5, 6, *Murex scolopax* Dillwyn, 1817. 7, 8, *Ringicula propinquans* Hinds, 1844. 9, 10, *Anadara antiquata* (Linnaeus, 1758). 11, 12, *Anadara uropigimelana* (Bory de St. Vincent, 1824). 13, 14, *Scapharca inflata* (Reeve, 1844). 15, 16, *Glycymeris livida* (Reeve, 1843). 17, 18, *Glycymeris* cf. *arabica* (H. Adams, 1871). 19, 20, *Modiolus auriculatus* (Krauss, 1848).

the beach face is steeper and plunging or surging waves are active. Under such circumstances, the surf zone narrows and shifts toward swash zone i.e shoreward with an increasing in depth (Wright et al., 1985). *Donax* cf. *bipartitus* (47.56%) tends to live in colonies at the edge of the surf zone or beyond offshore (Watson, 1971). In the present coastal segment, a noticeable mixing of bivalves *Donax* cf. *bipartitus* with *Mactra aequisulcata, Mactra lilacea*, and *Ringicula propinquans* which live in the surf zone, sandy offshore marine environment, together with shallower assemblages such as *Glycymeris livida*, *Glycymeris* cf. *arabica*, *Fulvia fragile, Anadara antiquata*, *Marcia flammea* and *Scapharca inflata* (Table 3) of shallow intertidal lower shoreface and muddy sands and shells attached to rocks in very shallow sea and/or lagoon such as *Brachidontes variabilis*, *Modiolus auriculatus, Hyotissa numisma* and *Saccostrea cucullata*

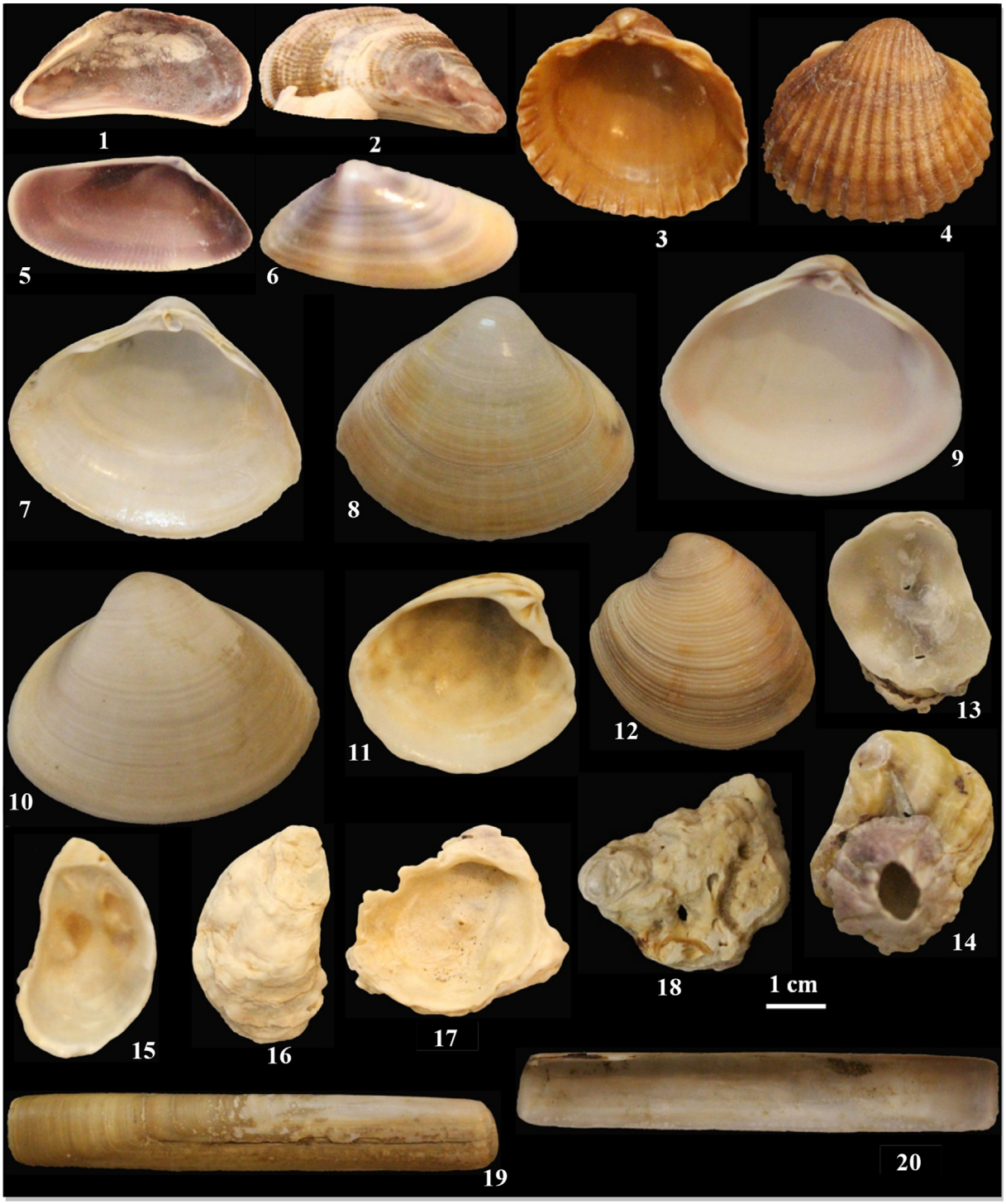

Fig. 12. 1, 2, *Brachidontes aariabilis* (Krauss, 1848). 3, 4, *Fulvia fragile* (Forrskàl, 1775). 5, 6, *Donax* cf. *bipartitus* Sowerby, 1892. 7, 8, *Mactra lilacea* Lamarck, 1818. 9, 10, *Mactra aequisulcata* Sowerby, 1894. 11, 12, *Marcia flammea* (Gmelin, 1791). 13, 14, *Hyotissa numisma* (Lamarck, l8l9). 15, 16, *Ostrea subucula* Lamy, 1925. 17, 18, *Saccostrea cuccullata* (Born, 1778). 19, 20, *Solen bravis* (Gray, 1842).

(Table 3). Such mixing suggests stormy conditions in a steepness and narrowness of the surf and swash zones, able to break and fragments the shell into pieces. Such storms never prevailed all over the year except in plunging wave breakings in an intermediate or reflective beach.

The present study clearly demonstrates the importance of implementation of coastal zone management strategy when dealing with the coastal hazards. It is important to stop constructing new heavy projects of oil and gas industries as well as petrochemical and logistic projects along the fragile segments of the coast. As most of these projects already have established, it is very important to look how we can secure the region in a scientific way. El-Asmar (1994) argued the strategy of the construction of the detached breakers to protect the resort houses without taking into

Table 3
Species, habitats and percent of the detected seashells along the study area.

Species	Habitats	Percent
Fulvia fragile	in muddy sand, lower shore and below	12.24
Donax cf. *bipartitus*	in sand, offshore	47.56
Neverita (Glossaulax) didyma	in sand	9.22
Mactra lilacea	in sand, offshore	4.75
Anadara antiquata	in muddy sand, intertidal and offshore	3.67
Marcia flammea	sand flats, intertidal	3.67
Glycymeris livida	in clean sand and gravel, shallow water	3.23
Glycymeris cf. *arabica*	in clean sand, shallow water	2.78
Mactra aequisulcata	in sand, offshore	2.60
Anadara uropigimelana	in sand, offshore	2.45
Ringicula propinquans	offshore to deep water and beached	2.14
Brachidontes variabilis	attached to stones and rocks or among rock oysters	1.83
Modiolus auriculatus	In shelly sand in crevices on rocky shores	1.38
Scapharca inflata	in sandy mud and mud in shallow waters	0.61
Hyotissa numisma	attached to rocks, mid-shore and below	0.45
Cerithidea cingulata	intertidal in sand	0.31
Saccostrea cuccullata	covering rocks, upper middle shore	0.31
Murex scolopax	in sand	0.16
Ostrea subucula	under rocks, upper middle shore	0.16
Solen brevis	offshore	0.47
Total		**100**

consideration the importance of the protection of the other strategic projects at the Damietta Harbor; such projects must have the priority in protection. He considered such way of construction of the detached breakwater system starting from Ras El-Bar westward in an opposite direction to the normal current as a technical mistake. Whatever the cost, it seems a vital and cheaper alternative is to extend the detached breakwater system to reach the eastern jetty of the Demiatta Harbor in order to secure the further coming projects as well as the recreational area Ras El-Bar extension to avoid categorizing as unsafe beaches (Zhiqiang, 2016).

5. Conclusions

Due to sediment entrapment after the construction of Aswan High Dam, the Nile Delta coast became no longer dissipative, divergent with a low-gradient. A subdivision into segments is here proposed in relation to shoreline direction toward induced waves and current, nature of sediments, and type of the implemented defense measures**.** Accordingly, the coastal strip between Ras El-Bar and the Damietta Harbor subdivided into two segments one to the east protected against erosion by detached breakwaters, the second to the west between the eastern jetty of the Damietta Harbor and the tip of the detached breakwaters system. The eastern segment is an accretional, gentle sloping, wide beach with fine to very fine sand enriched with heavy minerals and shows evidences of being a dissipative beach in divergent and spilling waves. The western one is erosional intermediate “d” beach, with shoreline retreat; steep slopping, cliffy, convergent and plunging breakings, with characteristic cuspate beach, rip currents, shell accumulation, reworked mud clasts, and discoidal gravels.

Shell accumulation in a convergence condition emphasized the presence of eddy waves resulted at the tip of the detached breaker system, creates the convergence conditions, lead to narrowing the surf and swash zone and mixing of shell assemblage.

An extension of the detached breakwater system is a must to protect private investments in real-estate of accommodations and hotels estimated in tens if not hundreds of billions at Ras El-Bar, beside the governmental taxes collected in due of such activities. Another kind of investments in free industrial zones, shipping and logistics, as well as gas industries along the Damietta Harbor should be also protected. The Damietta Harbor is expected to receive one of the Hub national projects for construction of the global logistics center for storage and handling of grain and cereals.

Acknowledgments

The authors would like to express their sincere appreciation to the Deanship of Scientific Research at King Saud University for funding this research group No. (RG-1435-033). Great thanks to Prof. Dr. Ahmed Basal, Department of Geology, Faculty of Science, Damietta University for supporting and fruitful discussion during the field work.

References

Aagaard, T., Hughes, M., Bladoch, T., Greenwood, B., Kroon, A., Power, H., 2012. Sediment transport processes and morphodynamics on a reflective beach under storm and non-storm conditions. Mar. Geol. 326–328, 154–165.
Aagaard, T., Greenwood, B., Hughes, M., 2013. Sediment transport on dissipative, intermediate and reflective beaches. Earth Sci. Rev. 124, 32–50.
Abo Zed, A.I., 2007. Effects of waves and currents on the siltation problem of Damietta Harbor, Nile Delta coast. Egypt. Mediterr. Mar. Sci. 8 (2), 33–47.
Alesheikh, A.A., Ghorbanali, A., Nouri, N., 2007. Coastline change detection using remote sensing. Int. J. Environ. Sci. Technol. 4 (1), 61–66.
Anderson, J.R., Hardy, E.E., Roach, J.T., Witmer, R.E., 1976. A land use and land cover classification system for use with remote sensor data. Geol. Surv.Profes. Paper 964, USGS, Reston, VA.
Arkhipenko, V.I., Gusakov, E.Z., Pisarev, V.A., Simonchik, L.V., 2002. Dynamics of the plasma wave breaking phenomena. In: 29th EPS Conference on Plasma Phys. And Contr. Fusion Montreux, ECA 26B, 5–09.
Asbury, H., Sallenger, J.R., 1979. Beach cusp formation. Mar. Geol. 29, 23–37.
A.S.R.T, 1988. Sedimentation in Damietta Harbour. Final report, Cairo, Egypt, 104 pp.
Braud, J.D.H., Feng, W., 1998. Semiautomated Constructions of the Lousiana Coastline Digital Land Water Boundary Using Landsat Thematic Mapper Satellite Imagery. Technical Report Series: 97–002, Louisiana.
Chander, G., Markham, B.L., Helder, D.L., 2009. Summary of current radiometric calibration coefficients for Landsat MSS, TM, ETM+, and EO-1 ALI sensors. Remote Sens. Environ. 113, 893–903.
Chanson, H., Lee, J.F., 1997. Plunging jet characteristics of plunging breakers. Coast. Engin 319 (1–4), 125–141.
Chavez, P.S., 1996. Image-based atmospheric correction—revised and improved. Photogram. Eng. Remote Sens. 62, 1025–1036.
Coco, G., O 'Hare, T.J., Huntley, D.A., 1999. Beach cusps: a comparisono f data and theories for their formation,. J. Coast. Res. 15, 741–749.
Coco, G., Huntley, D.A., O 'Hare, T.J., 2000. Investigation of a self-organization model for beach cusp formation and development. J. Geophys. Res. 105 (29), 21,991–22,002.
Davis, R., 1985. Coastal Sedimentary Environments, second ed. Springer Verlage. 731pp.
Dean, R.G., Dalrymple, R.A., 1991. Water Wave Mechanics for Engineering and Scientists. Advanced series on ocean engineering. 2. world scientific publishing company.
Deepika, B., Avinash, K., Jayappa, S., 2014. Shoreline change rate estimation and its

forecast: remote sensing, geographical information system and statistics-based approach Int. J. Environ. Sci. Technol. 11, 395–416.
Dennis, R.A., Colfer, C.P., 2006. Impacts of land use and fire on the loss and degradation of lowland forest in 1983–2000 in East Kutai District, East Kalimantan, Indonesia Singapore. J. Trop. Geogr. 27, 30–48.
Dewidar, Kh, 2004. Detection of land use/land cover changes for the northern part of the Nile delta (Burullus region), Egypt. Int. J. Remote Sens. 25 (20), 4079–4089.
Dewidar, Kh, 2011. Changes in the shoreline position caused by natural processes for coastline of Marsa Alam and Hamata, Red Sea. Egypt. Int. J. Geosci. 2, 523–529.
Dewidar, Kh, Frihy, O., 2010. Automated techniques for quantification of beach change rates using Landsat series along the North-eastern Nile Delta, Egypt. Journal of Oceanog. Mar. Sci. 1 (2), 28–39.
Eid, F.M., Sharaf El-Din, S.H., El-Din, K.A.A., 1997. Sea level variation along the Suez Canal. Estuarine, Coast. Shelf Sci. 44, 613–619.
El-Asmar, H.M., 1994. Severe coastal damage along Ras El-Bar shoreline, north of the Nile Delta: an effect of the construction of the detached breakwater system. J. Geol. Egypt 38 (2), 793–812.
El-Asmar, H.M., 1995. Impact of protection structures on physical and sedimentary parameters along the Damietta coastal area, Nile Delta, Egypt. J. Sedimentol., Egypt 3, 111–124.
El-Asmar, H.M., 2002. Short term coastal changes along Damietta–Port Said coast Northeast of the Nile Delta. Egypt. J. Coast.Res. 18 (3), 433–441.
El-Asmar, H., White, K., 1997. Updating of maps of dynamic coastal landforms by segmentation of thematic mapper imagery, examples from the Nile Delta, Egypt. In: Griffiths, G.H., Pearson, D. (Eds.), RSS97—Observations and Interactions. Proceedings of 23rd Annual Conference of the Remote Sensing Society. The University of Reading, Reading, UK, pp. 515–520, 2–4 September.
El-Asmar, H., White, K., 2002. Changes in coastal sediment transport processes due to construction of New Damietta Harbour, Nile Delta. Egypt Coast. Eng. 46, 127–138.
El-Asmar, H.M., Hereher, M., 2011. Change detection of the coastal zone east of the Nile Delta using remote sensing. Environ. Earth Sci. 62 (4), 769–777.
El-Asmar, H.M., Hereher, M., El-Kafrawy, S., 2012. Threats facing lagoons along the North Coast of the Nile Delta, Egypt. IJRA 2 (2), 24–29.
El-Asmar, H.M., Hereher, M., El-Kafrawy, S., 2013. Surface area change detection of the Burullus Lagoon, North of the Nile Delta, Egypt, using water indices: a remote sensing approach. Egypt. J. Remote Sens. Space Sci. 16, 119–123. http://dx.doi.org/10.1016/j.ejrs.2013.04.004.
El-Asmar, H.M., Taha, M.M.N., El-Kafrawy, S., 2014. Monitoring coastal changes along Damietta promontory and the barrier beach toward Port Said east of the Nile Delta. Egypt. J. Coast Res. 30 (5), 993–1005. http://dx.doi.org/10.2112/JCOASTRES-D-12-00112.1.
El-Banna, M.M., 2006. Responses of Ras El-Bar seafloor characteristics to protective engineering structures, Nile Delta. Egypt. Environ. Geol. 49, 645–652.
El-Banna, M.M., Hassaneen, N.N.A., 2002. Current pattern and bathymetry of Ras El-Bar resort behind the breakwater system. J. Env. Sci. Mans. Univ. Egypt 23, 119–132.
El-Dardir, M., 1994. Sedimentation in Nile High Dam reservoir 1987-1992 and sedimentary futurologic aspects. Sed. Egypt 2, 23–40.
El-Fishawi, N., 1994. Relative changes in sea level from tide gauge records at Burrulus, central part of the Nile Delta coast. INQUA MBSS Newsl. 16, 53–61.
Fanos, A.M., Khafagy, A.A., Dean, R.G., 1995. Protective works on the Nile Delta Coast. J. Coast. Res. 11, 516–528.
Foody, G., 2003. Remote sensing of tropical forest environments: towards the monitoring of environmental resources for sustainable development. Int. J. Remote Sens. 24, 4035–4046.
Frihy, O.E., Lawrence, D., 2004. Evolution of the modern Nile Delta promontories: development of accretional features during shoreline retreat. Environ. Geol. 46, 914–931.
Frihy, O.E., Deabes, E.A., 2011. Beach and nearshore morphodynamics of the central-bulge of the Nile Delta Coast, Egypt. IJEP 1 (2), 33–46.
Frihy, O.E., Fanos, A.M., Khafagy, A.A., Komar, P.D., 1991. Patterns of nearshore sediment transport along the Nile Delta, Egypt. Coast. Eng. 15, 409–429.
Frihy, O.E., Badr, A.A., Hassan, M.S., 2002. Sedimentation processes at the navigation channel of the Damietta harbour on the Northeastern Nile Delta coast of Egypt. J. Coast. Res. 18 (3), 459–469.
Frihy, O.E., Debes, E.A., El Sayed, W.R., 2003. Processes reshaping the Nile delta promontories of Egypt:pre- and post-protection. Geomorphology 53, 263–279.
Gad, M., Saad, A., El-Fiky, A., Khaled, M., 2013. Hydrodynamic modeling of sedimentation in the navigation channel of Damietta Harbor in Egypt. Coast. Eng. J. 55 http://dx.doi.org/10.1142/S0578563413500071.
Ghandour, I.M., Al-Washmi, H.A., Haredy, R.A., 2013. Gravel-sized mud casts on an arid microtidal sandy beach: example from the Northeastern Red Sea, South Al-Wajh, Saudi Arabia. J. Coast. Res. 29 (6a), 110–117.
Guneroglu, A., 2015. Coastal changes and land use alteration on Northeastern part of Turkey. Ocean Coast. Manag. 118, 225–233.
Hereher, M., 2014. The Lake Manzala of Egypt: an ambiguous future. Environ. Earth Sci. 72, 1801–1809. http://dx.doi.org/10.1007/s12665-014-3088-x.
Herold, M., Scepan, J., Clarke, K.C., 2002. The use of remote sensing and landscape metrics to describe structures and changes in urban land uses. Environ. Plan. 34, 1443–1458.
Holland, K.T., Holman, R.A., 1996. Field observations of beach cusps and swash motions. Mar. Geol. 134, 77–93.
Inman, D.L., Guza, R.T., 1982. The origin of swash cusps on beaches. Mar. Geol. 49, 133–148.
Jayson-Quashigah, P.N., Addo, K.A., Kodzo, K.S., 2013. Medium resolution satellite imagery as a tool for monitoring shoreline change. Case study of the Eastern coast of Ghana. J. Coast. Res. http://dx.doi.org/10.2112/SI65-087.1. Special Issue No. 65.
King, C.A.M., 1972. Beaches and Coasts. Edward Arnold, London, 573 pp.
Klemas, V., Abdel-Kader, A.M., 1982. Remote sensing of coastal processes with emphasis on the Nile Delta. In: Proceedings of the International Symposium on Remote Sensing of Environment, First Thematic Conference "Remote Sensing of Arid and Semi-arid Lands," January 19–25, Cairo, Egypt Ann Arbor, Michigan. Center for Remote Sensing and Information and Analysis, Environmental Research Institute, pp. 389–415.
Komar, P.D., 1971. Nearshore cell circulation and the formation of giant cusps. Geol. Soc. Am. Bull. 82, 2643–2650.
Komar, P.D., 1975. Nearshore currents–generation by obliquely incident waves and longshore variation in breaker height. In: Hails, J.R., Carr, A. (Eds.), Proceedings of the Symposium on Nearshore Sediment Dynamics. Wiley, New York, N.Y.
Komar, P.D., 1998. Beach Processes and Sedimentation, second ed. Prentice Hall, Upper Saddle River, NJ.
Lillesand, T.M., Kiefer, R.W., 1994. Remote Sensing and Image Interpretation. Wiley, New York.
Lillesand, T.M., Kiefer, R.W., Chipman, J.W., 2004. Remote Sensing and Image Interpretation. Wiley, New York.
Lorang, M.S., Stanford, J.A., Richard Hauer, F., Jourdonnais, J.H., 1993. Dissipative and reflective beaches in a large lake and the physical effects of lake level regulation. Ocean Coast. Manag 19, 263–287.
Lotfy, M.F., Frihy, O.E., 1993. Sediment balance in the nearshore zone of the Nile Delta coast. Egypt. J. Coast. Res. 9, 654–662.
Lopes, V., Pais-Barbosa, J., Taveira-Pinto, F., Veloso-Gomes, F., 2011. Beach cusps: using multivariate data analysis techniques for the identification of important variables and for predicting their spacing. J. Coast. Res. SI 64, 1106–1110.
Lu, D., Mausel, P., Brondizio, E., Moran, E., 2004. Change detection techniques. Int. J. Remote Sens. 25, 2365–2404.
Lunetta, R.S., Elvidge, C.D., 1998. Remote Sensing Change Detection: Environmental Monitoring Methods and Applications. Ann Arbor Press, Michigan.
Mahboob, M.A., Atif, I., 2016. Coastal change detection using moderate resolution satellite imagery: a case study of Makran coast, Arabian Sea, Pakistan. Sci. Int. (Lahore) 28 (1), 273–277.
Mass, J.F., 1999. Monitoring land-cover changes: a comparison of change detection techniques. Int. J. Remote Sens. 20, 139–152.
Masselink, G., Hegge, B.J., Pattiaratchi, C.B., 1997. Beach cusp morphodynamics. Earth Surf. Process. Landforms 22, 1139–1155.
Masselink, G., Pattiaratchi, C.B., 1998. Morphological evolution of beach cusps and associated swash circulation patterns. Mar. Geol. 146, 93–113.
Miles, J.R., Russell, P.E., 2004. Dynamics of a reflective beach with a low tide terrace. Cont. Shelf Res. 24, 1219–1247.
Mukherjee, S., Shashtri, S., Singh, C., Srivastava, P., Gupta, M., 2009. Effect of canal on land use/land cover using remote sensing and GIS. J. Indian Soc. Remote Sens. 37, 527–537.
Nafaa, M., Frihy, O.E., 1993. Beach and nearshore features along the dissipative coastline of the Nile Delta. Egypt. J. Coast. Res. 9 (2), 423–433.
Orlova, G., Zenkovich, V., 1974. Erosion of the shores of the Nile Delta. Geoforum 18, 68–72.
Ozturk, D., Sesli, F.A., 2015. Shoreline change analysis of the Kizilirmak Lagoon Series. Ocean Coast. Manag. 118, 290–308.
Pedrozo-Acuña, A., Torres-Freyermuth, A., Zou, Q., Hsu, T.J., Reeve, D.E., 2010. Diagnostic modelling of impulsive pressures induced by plunging breakers impinging on gravel beaches. Coast. Eng. 57 (3), 252–266.
Pedrozo-Acuña, A., Ruiz de Alegría-Arzaburu, A., Torres-Freyermuth, A., Mendoza, E., Silva, R., 2011. Laboratory investigation of pressure gradients induced by plunging breakers. Coast. Eng. 58 http://dx.doi.org/10.1016/j.coastaleng.2011.03.013, 722–238.
Pedrozo-Acuña, A., Resendiz, D., Mendoza, E., Silva, R., 2012. Sorting and beach morphology under plunging wave breaking. Coast. Eng. Proc. 33, 1–12.
Rao, V.R., Ramana Murthy, M.V., Manjunath, B., Reddy, N.T., 2009. Littoral sediment transport and shoreline changes along Ennore on the southeast coast of India: field observations and numerical modelling. Geomorphology 112, 158–166.
Santra Mitra, S., Santra, A., Mitra, D., 2013. Change detection analysis of the shoreline using Toposheet and Satellite Image: a case study of the coastal stretch of Mandarmani-Shankarpur, West Bengal, India. Intern. J. Geomatics Geosci. 3 (3), 425–437.
Serra, P., Pons, X., Saurı, D., 2003. Post-classification change detection with data from different sensors: some accuracy considerations. Int. J. Remote Sens. 24, 3311–3340.
Sestini, G., 1989. Nile Delta: a review of depositional environments and geological history. In: Whateley, M.K.G., Pikering, K.T. (Eds.), Deltas: Sites and Traps for Fossil Fuels, vol. 41. Blackwell Scientific Publications, Geological Society Special Publication, pp. 99–127.
Shalaby, A., Tateishi, R., 2007. Remote sensing and GIS for mapping and monitoring land cover and land-use changes in the Northwestern coastal zone of Egypt. Appl. Geogr. 27, 28–41.
Shepard, F.P., 1973. Submarine Geology, third ed. Harper & Row, New York.
Short, A.D., 2012. Coastal processes and beaches. Nat. Educ. Knowl. 3 (10), 15.
Smith, S.E., Abdel-Kader, A., 1988. Coastal erosion along the Egyptian delta. J. Coast.

Res. 4 (2), 245–255.
Sogreah, M., 1982. Effects on the Construction of the Port of Damietta on the Evolution of the Littoral Drift. Consultancy Report, number 35/1202/R9, 35 pp.
Srivastava, P.K., Han, D., Rico-Ramirez, M.A., Bray, M., Islam, T., 2012. Selection of classification techniques for land use/land cover change investigation. Adv. Space Res. 50 (9), 1250–1265.
Stanley, D.J., 1996. Nile delta: extreme case of sediment entrapment on a delta plain and consequent coastal land loss. Mar. Geol. 129, 189–195.
Tyagi, P., Bhosle, U., 2011. Atmospheric correction of remote sensed images in spatial and transform domain. Int. J. Image Process. 5 (5), 564–579.
Tetra Tech, 1984. Shoreline Master Plan for the Nile Delta Coast: Progress Report 1. Tetra Tech, Pasadena, California, 143pp.
Thornton, E.B., MacMahan, J., Sallenger Jr., A.H., 2007. Rip currents, mega-cusps, and eroding dunes. Mar. Geol. 240, 151–167.
Thieler, E.R., Himmelstoss, E.A., Zichichi, J.L., Miller, T.L., 2005. Digital Shoreline Analysis System (DSAS) Version 3.0: an Arc GIS Extension for Calculating Shoreline Change. U.S. Geological Survey Open File Report, 1304.
UNESCO/UNDP, 1978. Coastal Protection Studies. Final Technical Reportn1, 155 pp.
Van, T.T., Binh, T.T., 2008. Shoreline change detection to serve sustainable management of coastal zone in Cu long Estuary. In: Proceedings of the International Symposium on Geoinformatics for Spatial Infrastructure Development in Earth and Allied Sciences. Retrieved December 27, 2011 from. http://wgrass.media.osaka-cu.ac.jp/gisideas08/viewpaper.php?id=247.
Watson, R., 1971. Origin of shell beach. J. Sed. Petrol. 41 (4), 1105–1111.
White, K., El-Asmar, H.M., 1999. Monitoring changing position of coastlines using thematic mapper imagery, an example from the nile delta. Geomorph 29, 93–105.
Wright, L.D., Short, A.D., 1984. Morphodynamic variability of sufrf zones and beaches: a synthesis. Mar. Geol. 56, 93–118 93.
Wright, L.D., Chappell, I.J., Thom, B.G., Bradshawi, M.P., Cowell, P., 1979. Morphodynamics of reflective and dissipative beach and inshore systems: southeastern Australia. Mar. Geol. 32, 105–140.
Wright, L.D., Guza, R.T., Short, A.D., 1982. Dynamics of the high-energy dissipative surf. Mar. Geol. 45, 41–62.
Wright, L.D., Short, A.D., Green, M.O., 1985. Short term changes in the morphodynamic states of beaches and surf zones: an empirical predictive. Mar. Geol. 62, 339–364 339.
Yuan, F., Sawaya, K.E., Loeffelholz, B.C., Bauer, M.E., 2005. Land cover classification and change analysis of the Twin Cities (Minnesota) Metropolitan Area by multitemporal Landsat remote sensing. Remote Sens. Environ. 98, 317–328.
Zhiqiang, L., 2016. Rip current hazards in South China headland beaches. Ocean Coast. Manag 121, 23–32.